Cancer Cell
Article

TET2 Inactivation Results in Pleiotropic Hematopoietic Abnormalities in Mouse and Is a Recurrent Event during Human Lymphomagenesis

Cyril Quivoron,[1,2,3,14] Lucile Couronné,[1,2,3,14] Véronique Della Valle,[1,2,3,14] Cécile K. Lopez,[1,2,3] Isabelle Plo,[2,3,4] Orianne Wagner-Ballon,[4,5] Marcio Do Cruzeiro,[6] Francois Delhommeau,[4,7] Bertrand Arnulf,[8] Marc-Henri Stern,[9] Lucy Godley,[10] Paule Opolon,[3] Hervé Tilly,[11] Eric Solary,[2,3,4] Yannis Duffourd,[3] Philippe Dessen,[1,2,3] Hélène Merle-Beral,[12] Florence Nguyen-Khac,[12] Michaëla Fontenay,[13] William Vainchenker,[2,3,4] Christian Bastard,[11,15] Thomas Mercher,[1,2,3,15] and Olivier A. Bernard[1,2,3,15,*]

[1]INSERM, U985, Villejuif 94805, France
[2]Université Paris-Sud, Orsay 91400, France
[3]Institut Gustave Roussy, Villejuif 94805, France
[4]INSERM, U1009, Villejuif 94805, France
[5]Hôpital Henri Mondor, Créteil 94000, France
[6]Plateforme de Recombinaison Homologue, Institut Cochin, INSERM U1016; Centre National de la Recherche Scientifique (CNRS) Unité Mixte de Recherche (UMR) 8104; Université Paris Descartes, Faculté de Médecine Paris Descartes, 75014, Paris, France
[7]Université Pierre et Marie Curie, Hôpital Saint Antoine, Paris 75005, France
[8]A 3963, Université Paris VII, Hôpital Saint-Louis, Paris 75010, France
[9]INSERM, U830, Institut Curie, Paris 75005, France
[10]Department of Medicine, The University of Chicago, Chicago, IL 60637, USA
[11]INSERM, U918, Université de Rouen, Centre Henri Becquerel, Rouen 76038, France
[12]Service d'Hématologie Biologique, Hôpital Pitié-Salpêtrière, APHP; Université Pierre et Marie Curie-Paris 6; INSERM U872, Paris 75005, France
[13]Assistance Publique-Hôpitaux de Paris, Service d'Hématologie Biologique, Groupe Hospitalier Broca-Cochin-Hôtel-Dieu; Institut Cochin, Département d'Immuno-Hématologie, INSERM U1016, Centre National de la Recherche Scientifique (CNRS) Unité Mixte de Recherche (UMR) 8104, Université Paris Descartes, Faculté de Médecine Paris Descartes, Paris 75014, France
[14]These authors contributed equally to this work
[15]These authors contributed equally to this work
*Correspondence: olivier.bernard@inserm.fr
DOI 10.1016/j.ccr.2011.06.003

SUMMARY

Loss-of-function mutations affecting one or both copies of the *Ten-Eleven-translocation* (*TET*)*2* gene have been described in various human myeloid malignancies. We report that inactivation of *Tet2* in mouse perturbs both early and late steps of hematopoiesis including myeloid and lymphoid differentiation in a cell-autonomous manner, endows the cells with competitive advantage, and eventually leads to the development of malignancies. We subsequently observed *TET2* mutations in human lymphoid disorders. *TET2* mutations could be detected in immature progenitors endowed with myeloid colony-forming potential. Our results show that the mutations present in lymphoid tumor cells may occur at both early and later steps of lymphoid development and indicate that impairment of TET2 function or/and expression predisposes to the development of hematological malignancies.

Significance

TET2 mutations were associated with all subtypes of human myeloid malignancies. We show that Tet2 deficiency in mouse results in a cell-autonomous competitive advantage of hematopoietic progenitors, widespread hematological defects, and myeloid transformation. We also demonstrate that *TET2* mutations can be identified in human B and T cell lymphomas. These mutations can affect the hematopoietic stem cell compartment and may appear as an early event in the multistep process that leads to lymphoid or myeloid or both malignancies. These observations indicate that therapeutic strategies may have to target the hematopoietic stem cells to eradicate these diseases.

INTRODUCTION

Most human adult cancers develop through a multistep acquisition of a wide range of somatic mutations. It has been proposed that the tumor cells that initiate or maintain the malignant clone need to be able to self-renew. In human acute leukemia, this crucial property can be acquired by committed progenitors with limited self-renewal capacities through a genetic event or maintained through the targeting of hematopoietic stem cells (HSCs) (Cozzio et al., 2003; Goardon et al., 2011; Huntly et al., 2004). Leukemia-initiating cells are able to reconstitute the leukemia upon xenotransplantation in immunodeficient mice (Dick, 2008). Such cells have been experimentally shown to represent $1/10^2$–$1/10^6$ of the original blastic population in human acute myeloblastic and lymphoblastic leukemia. This notion, however, does not indicate the origin of the cell, namely, the cell in which the initial tumorigenic event occurred. Despite important progress in the identification of oncogenes involved in the development of human mature lymphoid malignancies, little is known regarding the initiating events in these diseases. More specifically, the natural history of mature T-lymphoid neoplasms is poorly understood (Jaffe, 2009; Jones, 2010).

The TET family proteins (Tet1, Tet2, Tet3) have been shown to catalyze the conversion of 5-methyl-cytosine (mC) to 5-hydroxymethyl-cytosine (hmC), a recently identified epigenetic mark (Ito et al., 2010; Koh et al., 2011; Kriaucionis and Heintz, 2009; Tahiliani et al., 2009). We and others have recently identified mutations in the *TET2* gene that frequently represent an early event during the development of a wide variety of human myeloid malignancies, including myeloproliferative neoplasms (MPNs), polycythemia vera (PV), essential thrombocythemia (ET), myelofibrosis (MF), myelodysplastic syndrome (MDS), chronic myelomonocytic leukemia (CMML), and acute myeloid leukemia (AML) (Abdel-Wahab et al., 2009; Delhommeau et al., 2009; Jankowska et al., 2009; Kohlmann et al., 2010; Kosmider et al., 2009a, 2009b; Langemeijer et al., 2009; Nibourel et al., 2010; Tefferi et al., 2009a, 2009b, 2009d). A correlation between low hmC and *TET2* mutation status was reported in patients with MDS (Ko et al., 2010b), suggesting that an altered 5-hydroxy-methylation status in promoter or imprinted region leads to deregulation of important hematopoietic regulators and participates to the malignant process.

In half of the patients, only one copy of *TET2* is mutated, arguing for a role of haploinsufficiency in transformation (Delhommeau et al., 2009; Langemeijer et al., 2009). The variety of myeloid disorders carrying a *TET2* mutation suggests that it may represent an early step in the transformation process, targeting the hematopoietic stem/progenitor cell compartment. *TET2* mutation may, however, also occur at late steps during the transformation of MPN to secondary acute leukemia (Abdel-Wahab et al., 2010; Beer et al., 2010; Couronné et al., 2010; Saint-Martin et al., 2009; Schaub et al., 2010).

To investigate the role of TET2 during hematopoiesis, we engineered two mouse models in which the 5-hydroxy-methylation function of Tet2 is impaired. In addition, we investigated the status of *TET2* coding sequences in various human mature lymphoid malignancies.

RESULTS

Murine Models of Tet2 Inactivation

We generated two *Tet2*-deficient mouse lines (Figure 1A). One was derived from a gene-trap ES clone (SIGTR ES cell line AN0709) in which a β-galactosidase-neomycin cassette was inserted in *Tet2* intron 9 ($Tet2^{LacZ}$ allele), thus leading to the expression of a Tet2-βGal fusion transcript (Figure 1A). We also generated a conditional knockout allele of *Tet2* in which the coding sequences of the last exon of *Tet2* are surrounded by *loxP* sites ($Tet2^{Lox}$). After Cre recombination, this allele results in the loss of the last 490 carboxy-terminal (Ct) amino acids of Tet2. In both models, *TET2* is predicted to lose the conserved Ct homology region of the double-stranded β-helix-2OG-Fe(II)-dependent dioxygenase domain. The two alleles were backcrossed for at least six generations into the C57BL/6 background, and then intercrossed to obtain homozygous animals.

Mice bearing the conditional *Tet2* allele and the interferon inducible Cre transgene (Mx1-Cre) were intercrossed to obtain a cohort of Mx1-$Cre^{+}Tet2^{Lox/Lox}$ (hereafter named $Tet2^{-/-}$) and control Mx1-$Cre^{-}Tet2^{Lox/Lox}$ (hereafter named $Tet2^{+/+}$) animals that were injected with poly(dI-dC) to induce Cre expression and acute inactivation of *Tet2* in adult animals. Full excision was observed in bone marrow and thymus (Figure 1B) and correlated with loss of normal *Tet2* mRNA expression in purified hematopoietic stem ($Lineage^{-}Sca\text{-}1^{+}c\text{-}Kit^{+}$: LSK cells) and progenitor populations (Figure 1C).

$Tet2^{LacZ/LacZ}$ animals were obtained at a Mendelian ratio, were fertile and appeared normal (data not shown). $Tet2^{LacZ/LacZ}$ progenitors showed a 20%–50% residual expression of a normal *Tet2* mRNA compared to wild-type progenitors, suggesting that the $Tet2^{LacZ}$ allele is an hypomorph allele (Figure 1D; see Figure S1 available online). Importantly, *Tet1* and *Tet3* expression levels remained unchanged in progenitors from both models (Figures 1C and 1D). Quantification of mC and 5hmC in $Tet2^{-/-}$ $lineage^{-}$ cells revealed a marked reduction of 5hmC compared to $Tet2^{+/+}$ (Figures 1E and 1F). Using a similar approach, no significant change in 5hmC level was detected in $Tet2^{LacZ/LacZ}$ $lineage^{-}$ cells (data not shown). Together these data confirmed the inactivation of *Tet2* in these models and indicate that loss of *Tet2* during adult hematopoiesis is not compensated by increased transcription of *Tet1* and *Tet3*.

Tet2 Controls Hematopoietic Stem and Progenitor Cells Homeostasis

Analysis of the hematopoietic compartments in these animals showed an amplification of the LSK compartment in 4- to 6-month-old animals in both *Tet2* inactivation models (Figures 2A and 2B; Figures S2A–S2D). Heterozygous animals also presented increased LSK in both models (Figures S3A and S3F). Within this compartment, $CD34^{+}Flt3^{-}$ short-term stem cells and to a lesser extent $CD34^{-}Flt3^{-}$ long-term stem cells were amplified. Notably, absolute numbers of $CD150^{+}CD48^{-}$ LSK cells were slightly increased (Figure 2A; Figure S2D). The absolute number of common myeloid progenitors (CMP) and megakaryocyte-erythrocyte progenitors (MEP) was increased, whereas the granulocyte-macrophage progenitor (GMP) population remained stable in $Tet2^{-/-}$ animals compared with controls

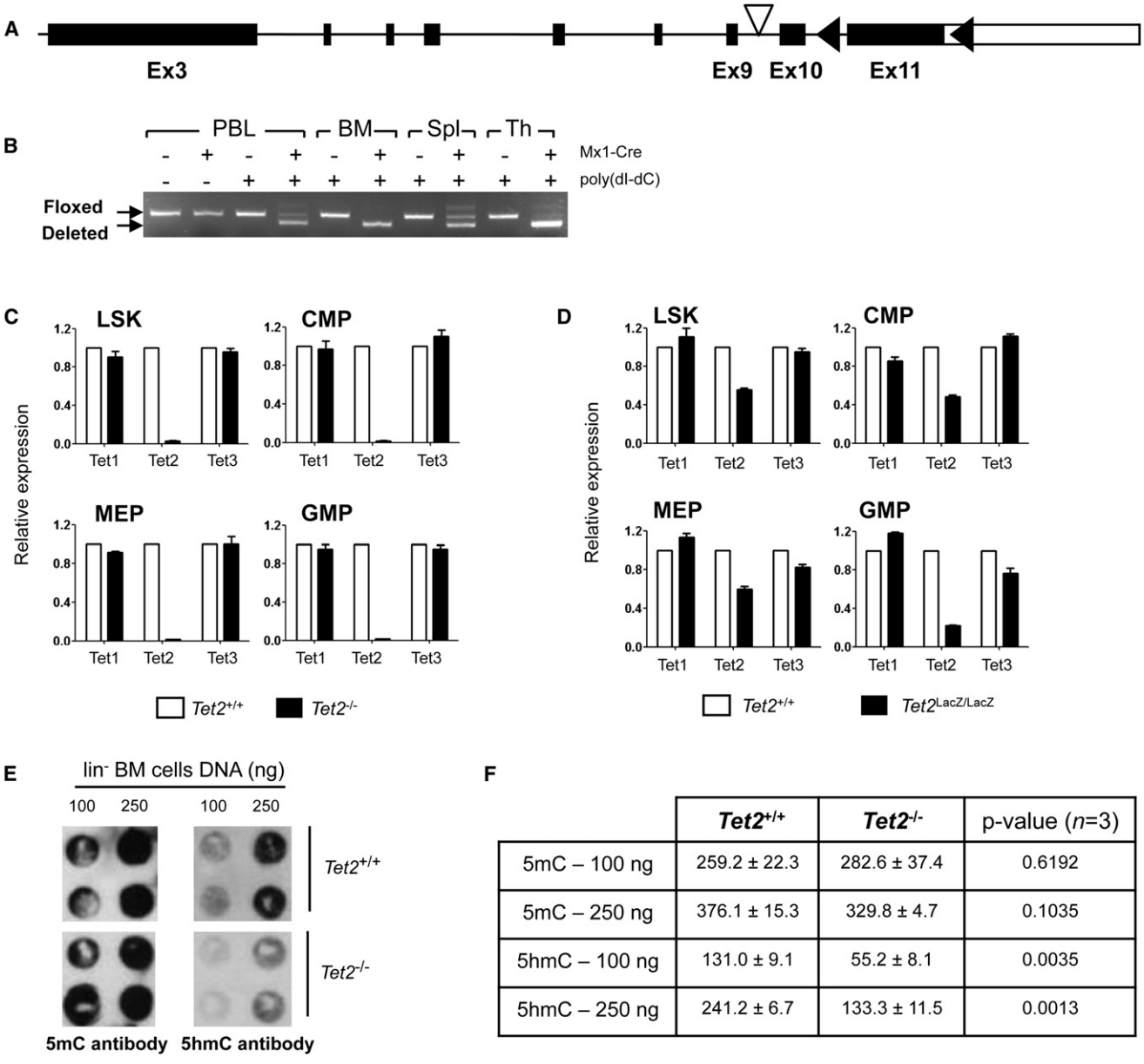

F

	Tet2$^{+/+}$	*Tet2*$^{-/-}$	p-value (*n*=3)
5mC – 100 ng	259.2 ± 22.3	282.6 ± 37.4	0.6192
5mC – 250 ng	376.1 ± 15.3	329.8 ± 4.7	0.1035
5hmC – 100 ng	131.0 ± 9.1	55.2 ± 8.1	0.0035
5hmC – 250 ng	241.2 ± 6.7	133.3 ± 11.5	0.0013

Figure 1. Description of the Two *Tet2* Inactivation Mouse Models

(A) Partial structure of the *Tet2* gene. For the *Tet2*^{LacZ} "LacZ" allele, the location of the gene-trap cassette containing a splice acceptor and a β-galactosidase-neomycin fusion gene is indicated (empty triangle). For the *Tet2*^{Lox} "floxed" allele, *loxP* sites (black triangles) have been introduced in intron 10 and in the 3′ untranslated region of exon 11.

(B) PCR analyses of Mx1-Cre-mediated exon 11 deletion in peripheral blood leukocytes (PBL), bone marrow (BM), spleen (Spl) and thymus (Th) cells from Mx1-Cre^{-}*Tet2*$^{Lox/Lox}$ (hereafter named *Tet2*$^{+/+}$) and Mx1-Cre^{+}*Tet2*$^{Lox/Lox}$ (hereafter named *Tet2*$^{-/-}$) animals 2 months after poly(dI:dC) injections (floxed allele: 305 bp; deleted allele: 237 bp).

(C) Quantitative RT-PCR analysis of expression of the murine *Tet1*, *Tet2* and *Tet3* genes in flow-sorted hematopoietic progenitors from *Tet2*$^{+/+}$ and *Tet2*$^{-/-}$ animals (n = 3 per genotype). Results are normalized with respect to *Abl1* expression and represented relatively to expression in control mice samples. *Tet2* RT-PCR assay spans the exon 10–11 boundary. LSK: Lin^{-}Sca-1^{+}c-Kit^{+}; CMP: common myeloid progenitor; MEP: megakaryocyte-erythrocyte progenitor; GMP: granulocyte-macrophage progenitor.

(D) Quantitative RT-PCR analysis in *Tet2*$^{LacZ/LacZ}$ versus wild-type controls as in C (n = 3 per genotype).

(E) Drop in 5-hydroxymethyl-cytosine (5hmC) in immature populations of *Tet2*-inactivated mice. Immunoblot analyses of increased quantity of genomic DNA from BM lineage (lin)-negative cells of *Tet2*$^{+/+}$ and *Tet2*$^{-/-}$ mice 4 months after poly(dI:dC) induction using anti 5-methylcytosine- (5mC) antibody (left panel) and 5-hydroxymethyl-cytosine- (5hmC) antibody (right panel).

(F) Quantification of the signal shown in (E).

See also Figure S1.

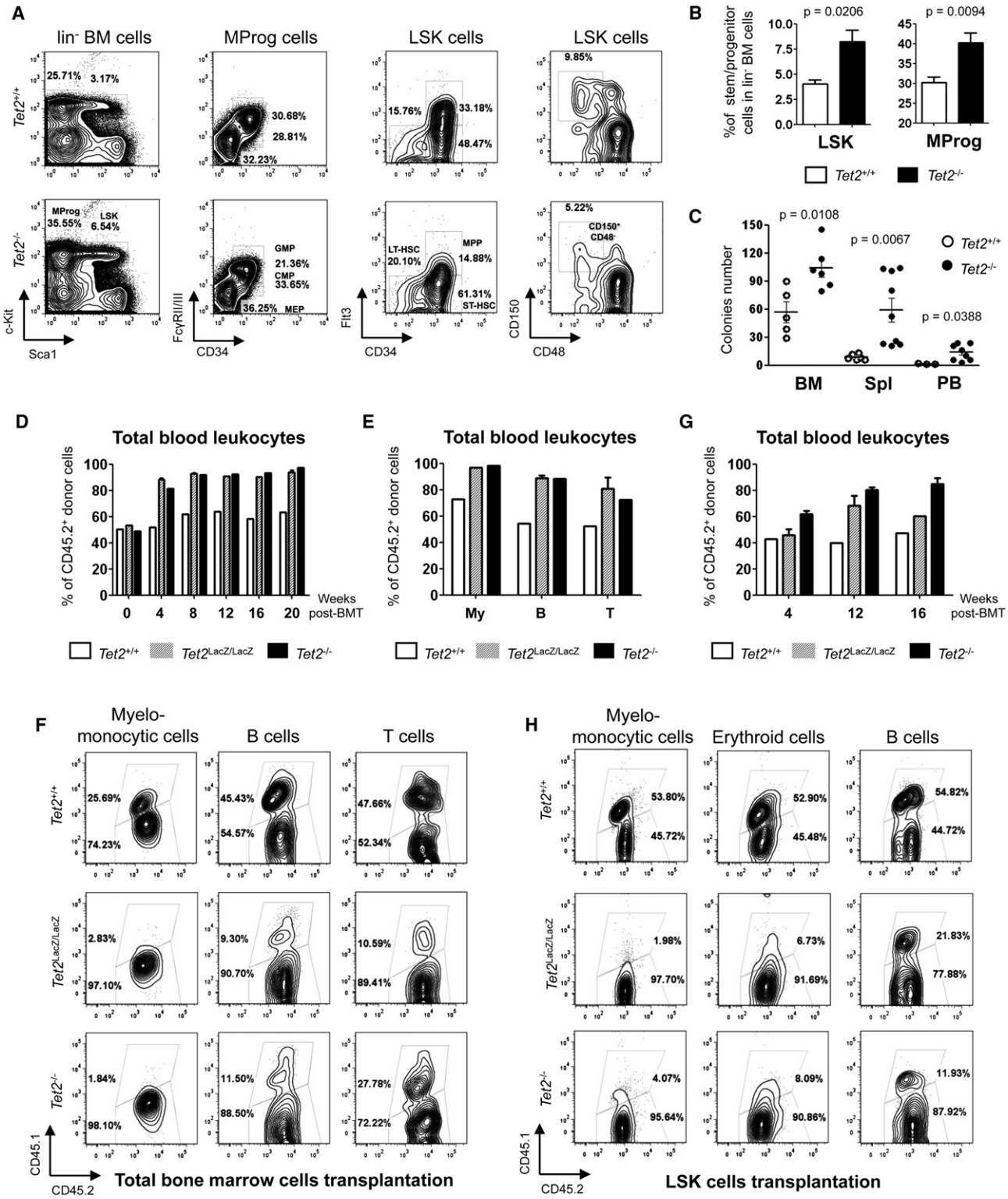

Figure 2. Tet2 Regulates Hematopoietic Stem and Progenitor Compartments Homeostasis

(A) Flow cytometrical analysis of hematopoietic stem and progenitor cells in the bone marrow of *Tet2*$^{+/+}$ and *Tet2*$^{-/-}$ animals. Analysis was performed 4–6 months postinduction. Percentages within lineage$^-$ bone marrow cells (left panel), myeloid progenitor cells (MProg: lin$^-$Sca-1$^-$c-Kit$^+$ cells; middle left panel), or within LSK cells (lin$^-$Sca-1$^+$c-Kit$^+$ cells; middle right and right panel) are indicated.

(B) Representation of the results exemplified in A as a percentage of lineage-negative hematopoietic progenitors. Data are presented as mean ± SEM *Tet2*$^{+/+}$ (n = 6; white histogram) and *Tet2*$^{-/-}$ (n = 6; black histogram) mice.

(Figures S2E and S2K). Bone marrow cells from *Tet2*$^{-/-}$ animals presented a functional increase in methylcellulose colony forming progenitors (Figure 2C; Figures S2F and S2G). Of note, the average number of cells per colony was higher in *Tet2*-deficient cell cultures compared with controls (Figures S2F and S2M). Culture of purified LSK cells from some *Tet2*$^{-/-}$ animals 12 months after induction also produced an increased number of cells presenting a decreased differentiation toward CD11b^{+}Gr1^{+} myeloid cells and a higher maintenance of the immature c-Kit^{+}Sca1^{+} phenotype compared with controls (Figures S2H and S2I). The amplitude of this phenotype was variable among animals. Similar results were obtained from gene-trap animals (Figures S2J–S2N).

To demonstrate the cell-autonomous nature of this property, we transplanted total bone marrow or purified LSK cells from both *Tet2*-deficient models (CD45.2^{+}CD45.1^{-}) in competition with wild-type cells (CD45.2^{+}CD45.1^{+}) into wild-type CD45.2^{-}CD45.1^{+} recipients. Homozygous *Tet2*-deficient cells from both models efficiently reconstitute all hematopoietic lineages for over 16 weeks, indicating that amplified LSK cells are functional (Figures 2D–2H; Figures S2O–S2S). In both myeloid and lymphoid lineages, the contribution of *Tet2*-deficient cells progressively increased over that of wild-type cells. An amplification of the LSK compartment was observed in some recipient animals (Figure S2R).

Together, these data showed that Tet2 inactivation resulted in a phenotypic and functional amplification and a competitive advantage of hematopoietic stem and progenitor cells indicating cell-autonomous control of their homeostasis by Tet2.

Tet2 Inactivation Induces Alteration of Several Mature Hematopoietic Lineages

To further characterize the consequences of Tet2 inactivation on mature hematopoietic lineages, we followed a cohort of *Tet2*$^{-/-}$, *Tet2*$^{LacZ/LacZ}$ animals and their respective controls for disease development. Four-month-old *Tet2*$^{-/-}$ and *Tet2*$^{LacZ/LacZ}$ animals present a modest increase in white blood cell counts, a decrease in erythroid and platelets counts, and a significant hepatosplenomegaly compared with controls (Figures 3A and 3B; Figures S3H and S3I). Histopathological analysis showed an alteration of the normal splenic architecture with significant expansion of the red pulp and infiltration of the lymphoid follicles with admixed maturing myeloid, immature erythroid, and maturing megakaryocytic elements (Figure S3L; Figure 3C). Analysis of the liver showed that *Tet2*$^{-/-}$ animals presented a diffuse infiltration of the sinusoids with an admixture of lymphoid and trilineage myeloid elements with some focused perivascular infiltrations (Figure S3L).

Flow cytometrical analysis confirmed an amplification of myeloid cells in both models with a marked increase in a myelomonocytic CD11b^{+}Gr1^{-} population in the peripheral blood and spleen (Figure 3D). Alteration of the erythroid lineage was observed in the bone marrow with a significant increase in CD71^{+}Ter119^{-} proerythroblasts and a decrease in the number of CD71^{low}Ter119^{+} late erythroblasts (Figure 3E). Splenic erythropoiesis was also visible with an increase in the number of CD71^{+}Ter119^{+} erythroid cells (Figure 3E). Tet2-deficient splenocytes could form multilineages colonies in methylcellulose colony-forming assays confirming extramedullar hematopoiesis (Figure 2C and data not shown). Similar abnormalities were observed in the gene-trap model (Figures S2M, S2N, S3J, and S3K).

Lymphoid lineages were also affected with a global increase in the number of immature double-negative (DN) CD4^{-}CD8^{-} T cell progenitors in the thymus, more particularly, CD44^{+}CD25^{-} DN1 cells (Figure 3F; Figures S3Q–S3V). The B cell lineage was also altered with a decreased number of bone marrow B220^{+}IgM^{-} pre- and pro-B cells and B220^{+}IgM^{low} mature B cells (Figure 3G) associated with an increase in the number of splenic B cells (Figure 3H; Figures S3M–S3P). Of note, heterozygous *Tet2*$^{LacZ/wt}$ animals present similar abnormalities of the myeloid, erythroid and B cell lineages (Figure S3B). Also, both lymphoid and myeloid lineage alterations were observed in recipients of *Tet2*-deficient cells (Figure S2O), indicating that differentiation abnormalities are cell autonomous.

With age, some *Tet2*$^{LacZ/wt}$ and *Tet2*$^{LacZ/LacZ}$ animals developed a lethal phenotype associated with important weight loss, high white blood cell counts, anemia, thrombocytopenia, and massive hepatosplenomegaly (Figures 4A and 4B; data not shown). Histopathological analysis of moribund animals showed complete effacement of the spleen architecture and massive perivascular as well as interstitial infiltration of the liver with myeloid elements (Figure 4C). A moderate fibrosis, assessed by increased reticulin fiber staining on tissue sections, was observed in the spleen and liver but not the bone marrow (Figure 4D). Flow cytometrical analysis confirmed the myeloid and erythroid lineage hyperplasia with abnormal myelomonocytic differentiation revealed by a striking amplification of the CD11b^{+}Gr1^{-} population visible in younger Tet2-deficient animals (Figure 4E). Importantly, the disease was transplantable to

(C) Clonogenic activity of bone marrow (BM), spleen (Spl) and peripheral blood (PB) cells from *Tet2*$^{+/+}$ (n = 6; white circles) and *Tet2*$^{-/-}$ (n = 6; black circles) mice 4–8 months postinduction in methylcellulose M3434 medium. Colonies were scored after 7 days and results are represented as mean colony number ± SEM. See also Figure S2.

(D) Competitive bone marrow transplantation (BMT) assay. CD45.2^{+} donor BM cells isolated from *Tet2*$^{+/+}$, *Tet2*$^{LacZ/LacZ}$ and *Tet2*$^{-/-}$ mice were transplanted into lethally irradiated CD45.1^{+} recipients, in equivalent number to wild-type competitor CD45.1^{+}CD45.2^{+} BM cells. The percentage of donor chimerism (CD45.2^{+} cells) in the blood is given at the indicated time points post-BMT (n = 2 mice per genotype). See also Figure S2.

(E) Percentage of CD45.2^{+} donor chimerism in blood cells 20 weeks post-BMT; myelomonocytic cells (My; CD11b^{+}Gr-1^{+}), B cells (CD19^{+}B220^{+}) and T cells (CD4^{+} or CD8^{+}). Values shown are mean ± SEM (n = 2 mice per genotype).

(F) Representative flow cytometrical profiles of donor chimerism in blood subpopulations shown in (E) (host cells were electronically excluded with CD45.1).

(G) LSK cells transplantation. CD45.2^{+} sorted-LSK cells isolated from *Tet2*-deficient or wild-type mice were transplanted into lethally irradiated CD45.1^{+} congenic recipients. The percentage of donor chimerism in the blood is given at the indicated time points post-BMT. Values shown are mean ± SEM (n = 2 mice per genotype). See also Figure S2.

(H) Representative flow cytometrical analysis of donor chimerism in bone marrow subpopulations 16 weeks post-BMT (CD11b^{+}Gr-1^{+} myelomonocytic cells; CD71^{+} erythroid cells; CD19^{+}B220^{+} B cells).

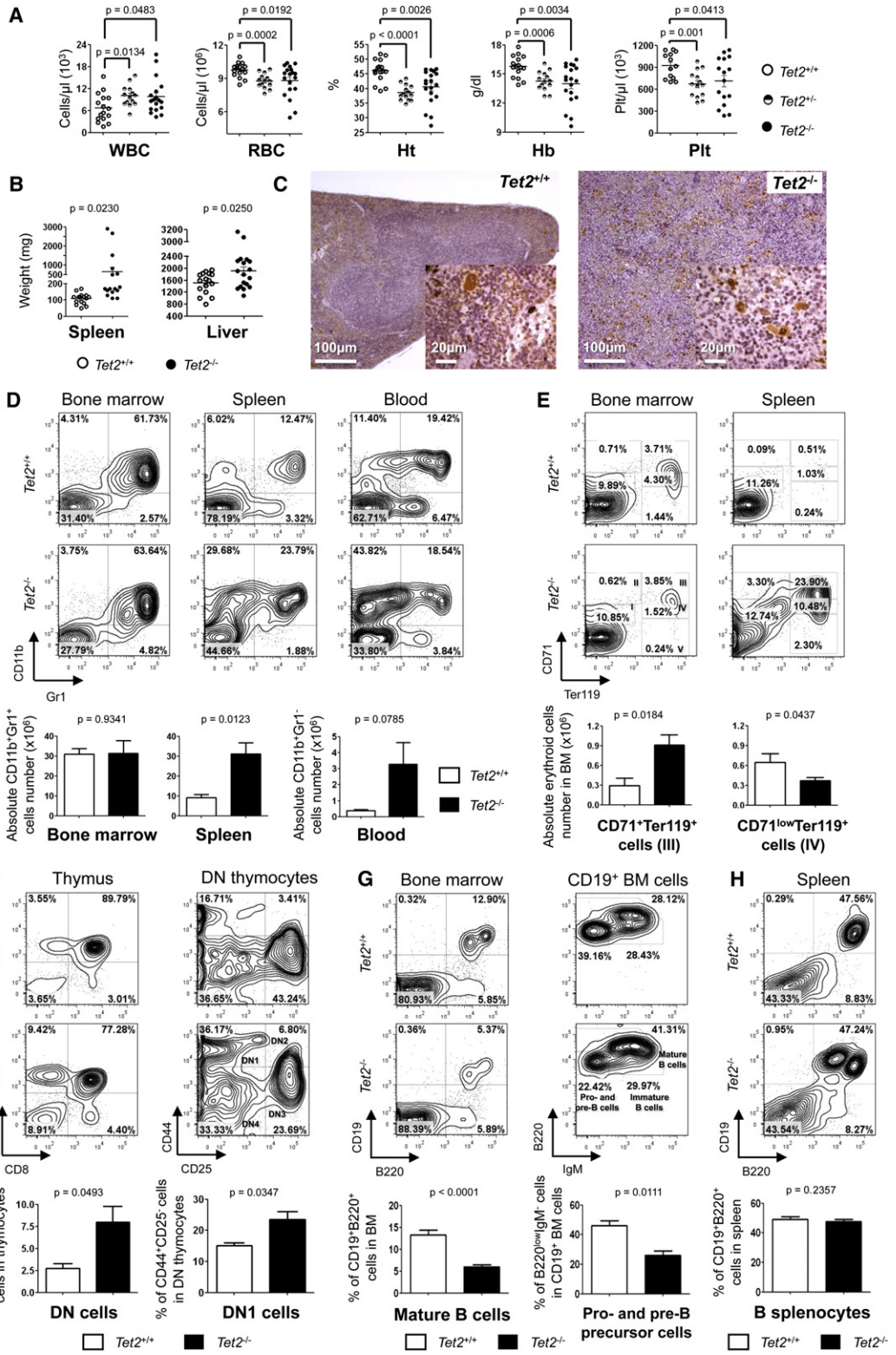

Figure 3. Tet2 Inactivation Results in Aberrant Myeloid and Lymphoid Maturation

(A) White blood cell (WBC), red blood cell (RBC), hematocrit (Ht), hemoglobin (Hb), and platelet (Plt) counts in peripheral blood samples obtained from *Tet2*$^{+/+}$, *Tet2*$^{+/-}$, and *Tet2*$^{-/-}$ mice, performed 4–6 months postinduction. See also Figure S3 and Table S1.

(B) Spleen and liver weights of mutant and littermate control mice.

(C) Von Willebrand staining on spleen sections from *Tet2*$^{+/+}$ and *Tet2*$^{-/-}$ animals highlights megakaryocytic hyperplasia in *Tet2*$^{-/-}$ animals 4 months postinduction.

secondary recipients, which succumbed with a shorter latency and a similar phenotype (Figure S4). To date, *Tet2*$^{-/-}$ animals did not develop lethal disorders with a follow-up of over 15 months.

Together, these results show that *Tet2* inactivation in mice results in pleiotropic alterations of the immature and mature hematopoietic compartments including both lymphoid and myeloid lineages (summarized in Table S1). With time, *Tet2* inactivation leads to bona fide myeloid malignancies with differentiation abnormalities reminiscent of human CMML.

TET2 Is Mutated in Human Lymphoid Malignancies

Based on these results indicating that TET2 controls both self-renewal and/or proliferation of early progenitors and also late steps of both myeloid and lymphoid hematopoietic differentiation, we investigated whether human lymphoid malignancies could also present *TET2* mutations. Supporting this hypothesis, two of six patients presenting myeloid malignancies and initially investigated for *TET2* alterations, concomitantly suffered from lymphomas (Delhommeau et al., 2009; Viguié et al., 2005). Therefore, we resequenced the entire coding sequence of *TET2* in a series of human lymphoid malignancies. No nucleotide changes inducing truncation or aminoacid changes in the catalytic domain of TET2 were observed in chronic lymphocytic leukemias (CLLs) (n = 75), plasma cell neoplasms (PCNs) (n = 22), and leukemic or disseminated T cell neoplasms (n = 45) [including T cell prolymphocytic leukemia (TPLL), T cell large granular lymphocytic leukemias (TGLLs), and adult T cell lymphoma/leukemia HTLV1+ (ATLL HLTV1)]. In a series of 301 B cell lymphoma and 177 T cell lymphoma samples, *TET2* mutations were observed in 2.0% of B cell and 11.9% of T cell lymphomas and in up to a third of the angioimmunoblastic T cell lymphoma (AITL) samples (Table 1). The mutations were mainly insertion/deletions, generating frameshifts and nonsense mutations, as seen for myeloid malignancies (Table S2). Of note, five of these patients had a known history of successive hematological malignancies (Table S3).

We also analyzed T-lymphoma samples by DNA micro-arrays, including nine *TET2* wild-type and ten *TET2* mutated samples. The analysis revealed that one of the mutated samples also exhibited a small genomic deletion of chromosome 4q including the *TET2* locus (Figure S5A). Therefore, as for myeloid malignancies, *TET2* genomic abnormalities are less frequent than *TET2* mutations but may occur in conjunction.

Matched nontumoral DNA samples were available for 13 patients with *TET2* mutations (Figure 5A, Table S2, Figures S5B and S5C). The TET2 sequences were wild-type in two patients (patients 5 and 6). The mutated TET2 sequence detected in the lymphoma cells was clearly observed in the nontumoral DNA samples of five patients (patients 3, 4, 13, 15, and 26). In two of them (patients 3 and 15), this might be due to the presence of tumor cells, as judged by PCR analyses for TCR or IgH clonality or the presence of IGH-BCL2 fusion transcript (data not shown). Trace of the mutated TET2 sequence was suspected in six matched samples (patients 2, 10, 16, 17, 20, and 21) of which three (patients 2, 10, and 16) were devoid of tumor cells. Mutations observed in patients 17, 20, and 25 have been described as acquired in myeloid malignancies.

Together the mutated *TET2* sequences were observed in the matched sample despite the absence of detectable circulating tumor cells in five samples (patients 2, 4, 10, 13, and 16). In two of these samples (patients 4 and 13), the estimated burden of mutated sequences was comparable to the wild-type sequence. Two hypotheses could account for these observations: either the mutation was germline transmitted, or the mutation was acquired and had endowed the clone with a growth advantage over wild-type progenitors, leading to a skewed hematopoiesis.

TET2 Mutations Are Detected in CD34^{+} Cells with Myeloid Potential

To test the hypothesis that *TET2* mutations may arise in early hematopoietic progenitors in patients presenting lymphomas, we analyzed three patients for which viable cells were available. Patient 8 was diagnosed with an AITL and carried a Q1445X mutation. Blood mononuclear cells were grown in a colony assay supporting myeloid differentiation. Of the 11 colonies that grew out, 5 showed only a wild-type *TET2* allele and 6 showed both Q1445X and wild-type alleles (Figure 5B). These results demonstrate the acquired nature of the *TET2* mutation in this patient and also indicate its presence in progenitor cells with myeloid colony-forming potential.

Patient 2 was initially diagnosed with a B cell lymphoma carrying two *TET2* mutations [(E448fs; 4663+1G > A: splice site mutation)] that were barely detectable in blood sample (Figure 5C). Five months after treatment, the patient developed an MDS that rapidly evolved into AML. Viable bone marrow cells were available only at the AML phase. DNA was extracted from whole bone marrow cells, purified CD34^{-} and CD34^{+} fractions.

(D) Representative flow cytometrical analysis of the mature myeloid cells in the bone marrow, spleen, and blood of *Tet2*$^{+/+}$ and *Tet2*$^{-/-}$ animals. Percentages of total cells are indicated. Lower panel: absolute number of cells from analysis shown in (C). *Tet2*$^{+/+}$ (n = 10; white bars) and *Tet2*$^{-/-}$ (n = 16; black bars) animals are represented as mean ± SEM. See also Table S1.

(E) Representative flow cytometrical analysis of the erythroid lineage in the bone marrow and spleen of *Tet2*$^{+/+}$ and *Tet2*$^{-/-}$ animals. Percentage of total cells is indicated. Lower panel: absolute number of cells from analysis shown in (D). *Tet2*$^{+/+}$ (n = 10; white bars) and *Tet2*$^{-/-}$ (n = 16; black bars) animals are represented as mean ± SEM.

(F) Representative flow cytometry analysis of thymocytes in *Tet2*$^{+/+}$ and *Tet2*$^{-/-}$ mice performed 4 months postinduction. Upper left panels: the percentages of total thymocytes are indicated. Upper right panels: the percentages of thymocytes precursors in Lineage^{-}CD4^{-}CD8^{-} double-negative (DN) cells are represented. Lineage antibodies included antibodies against CD19, CD3ε, CD8, TCR-β, NK-1.1, Ly-6G, and CD11b murine markers. Lower panels: the percentages of CD4^{-}CD8^{-} DN in total thymocytes and CD44^{+}CD25^{-} DN1 cells in DN precursor thymocytes from *Tet2*$^{+/+}$ and *Tet2*$^{-/-}$ animals (n = 3 per genotype) are represented as mean ± SEM. See also Figure S3.

(G) Flow cytometrical analysis of B cells in the bone marrow of *Tet2*$^{+/+}$ and *Tet2*$^{-/-}$ animals 4 months postinduction. Left panel: whole bone marrow. Right panel: gated on CD19^{+} cells (the frequencies are indicated as a percentage of CD19^{+} cells). Gates include pro- and pre-B precursor cells (B220^{low} IgM^{-}), immature B cells (B220^{low} IgM^{hi}) and mature B cells (B220^{hi} IgM^{hi}). Lower panels indicate mean ± SEM of eight animals per genotype. See also Table S1.

(H) Flow cytometrical analysis of splenic B cells in *Tet2*$^{+/+}$ and *Tet2*$^{-/-}$ animals. Lower panel indicate mean ± SEM of ten animals per genotype.

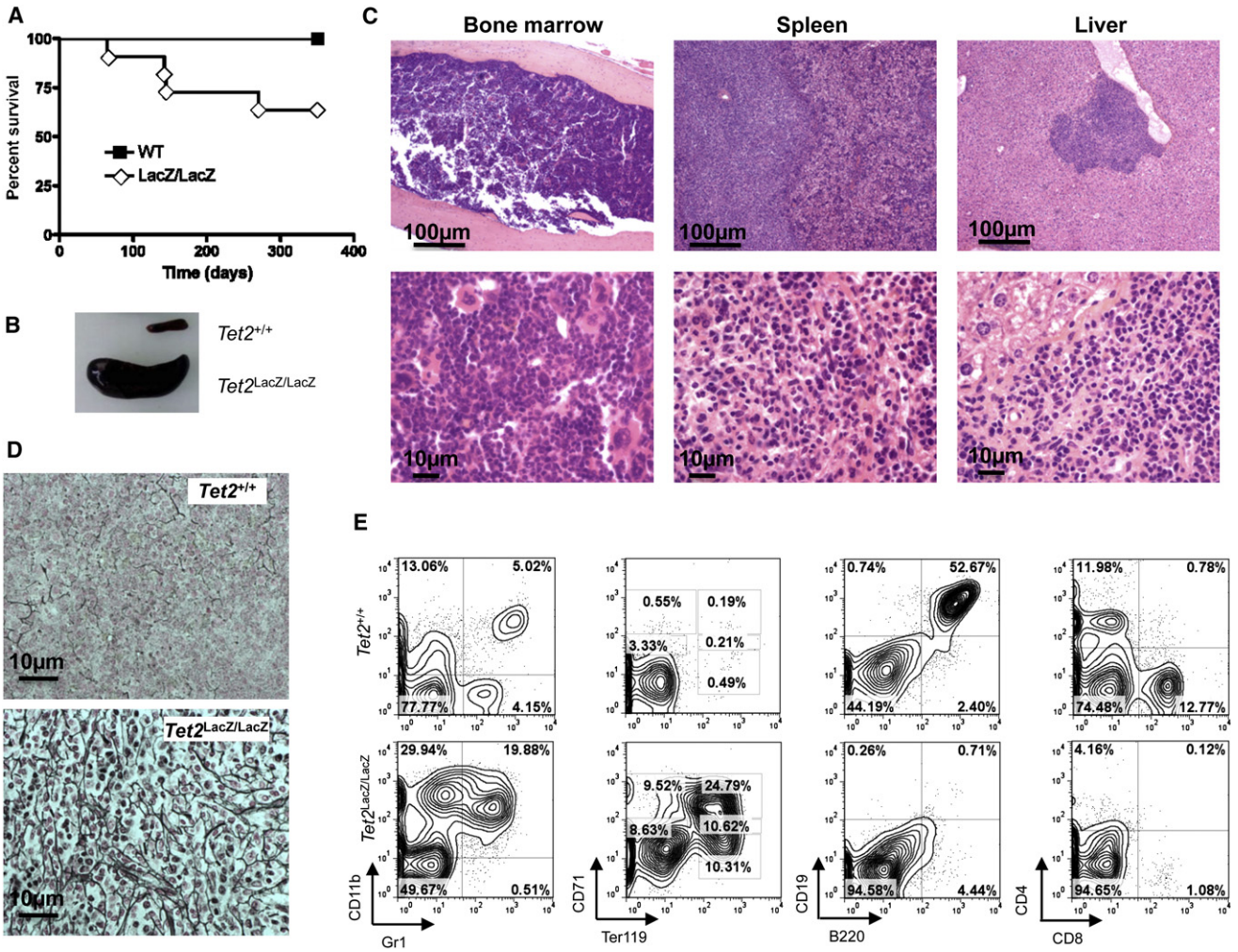

Figure 4. Tet2 Inactivation Induces Fatal Hematopoietic Malignancies

(A) Kaplan-Meier survival curve of *Tet2*$^{LacZ/LacZ}$ animals and wild-type littermate controls. Only animals that reached moribund state were considered. See also Figure S4.

(B) Representative picture of spleens observed in mutant *Tet2*$^{LacZ/LacZ}$ mouse compared with spleens from wild-type littermates.

(C) Hematoxylin-Eosin-Safran (HES) staining of bone marrow, spleen and liver sections from a 14-month-old moribund *Tet2*$^{LacZ/LacZ}$ animal. See also Figure S3L.

(D) Reticulin staining of spleen from animal in (C).

(E) Flow cytometrical analysis of myelomonocytic, erythroid, B and T lymphoid lineages in the spleen of a 14-month-old moribund mutant *Tet2*$^{LacZ/LacZ}$ mouse. Of note, this animal displayed leukocytosis (69.1 × 10^6 WBC/mm^3), anemia (1.76 × 10^6 RBC/mm^3, 12.6% hematocrit, and 4.7 g hemoglobin/dl), thrombocytopenia (189 × 10^3 platelets/mm^3) and hepatosplenomegaly (liver and spleen weights were 3960 and 2000 mg, respectively). See also Figure S4.

In every DNA samples, both *TET2* mutations were observed at seemingly variable ratios with respect to the wild-type sequence. DNA was extracted from 28 colonies grown in myeloid conditions in vitro, from single CD34$^+$ cells. Six colonies showed only wild-type *TET2* sequences, 14 colonies presented both *TET2* mutations, and 8 colonies carried only the splice site mutation (Figure 5C). These data demonstrate the presence of *TET2* mutations in both the lymphoma and the AML cells, confirmed their acquired nature. Taken together, these observations suggest that the *TET2* mutated clone had invaded the bone marrow and was at the origin of both the lymphoid and myeloid type malignancies.

Patient 27 was diagnosed with a T cell lymphoma. Bone marrow aspirate examination was cytologically normal. We observed two *TET2* mutations (P761fs and Q481X) in the CD34$^-$CD3$^-$CD19$^-$CD14$^-$ cell fraction (the remaining fraction after successive exclusion of the CD3$^+$, CD19$^+$ and CD14$^+$ cell fractions from the blood sample), which were absent in the other fractions (Figure 6A). In vitro colonies assay of sorted CD34$^+$ cells showed the presence of P761fs in 6 of 84 (~7%) colonies, whereas the stop mutation was not observed (Figure 6C). This fraction remained stable, since a similar analysis showed 6 out of 93 (~6.5%) colonies with the P761fs mutation 4 months later. Of the 45 colonies obtained from cultures of Lineage$^-$CD34$^+$ CD38$^-$ sorted cells, only one carried the P761fs (Figure 6C). These results show the acquired nature of the *TET2* mutations in this patient and indicate the presence of a *TET2* mutation on one copy in a small fraction of hematopoietic progenitors with myeloid differentiation potential.

Table 1. TET2 Mutations in B and T Cell Neoplasms

B cell ceoplasms	All patients	Mutated TET2
LPL	2	0 (0%)
PCN	22	0 (0%)
CLL /SLL	75	0 (0%)
TCRBL	3	0 (0%)
DLBCL	87	5 (5.7%)
MCL	22	0 (0%)
MZL	17	0 (0%)
FL	68	1 (1.5%)
Unspecified B-lymphoma	5	0 (0%)
Total	301	6 (2.0%)
T cell neoplasms	All patients	Mutated TET2
TLBL	5	1 (20%)
Leukemic or disseminated (TPLL, TGLL, ATLL)	45	0 (0%)
Extranodal (ETCL, hepatosplenic)	4	0 (0%)
Extranodal cutaneous (Sezary, MF…)	42	2 (4.8%)
AITL	30	10 (33.3%)
ALCL	8	0 (0%)
PCTL, NOS	30	6 (20%)
Unspecified T-lymphoma	13	2 (15.4%)
Total	177	21 (11.9%)

LPL, lymphoplasmacytic lymphoma (including Waldenström macroglobulinemia); PCN, plasma cell neoplasms (including plasma cell myeloma and plasma cell leukemia); CLL, chronic lymphocytic leukemia; SLL, small lymphocytic lymphoma; TCRBL, T cell-rich B cell lymphoma; DLBCL, diffuse large B cell lymphoma; MCL, mantle cell lymphoma; MZL, marginal zone lymphoma; FL, follicular lymphomal; TLBL: precursor T-lymphoblastic lymphoma; TPLL, T cell prolymphocytic leukemia; TGLL, T cell large granular lymphocytic leukemia; ATLL, adult T cell lymphoma/leukemia (HTLV1+); ECTL, enteropathy-associated T cell lymphoma; MF, mycosis fungoides; AITL, angioimmunoblastic T cell lymphoma; ALCL, anaplastic large cell lymphoma; PCTL-NOS, peripheral T cell lymphoma not otherwise specified.

Taken together, these results show the presence of *TET2* mutations in B and T cell lymphomas. Detailed analysis of three patients indicated that lymphoma cells carried one somatic mutation originally acquired in an hematopoietic stem cell. During T cell maturation/differentiation, a second *TET2* mutation may occur, leading to the total loss of TET2 function in lymphoma cells.

To investigate the sequence of events occurring during tumor development, we further analyzed the tumor cells from patient 27. SNP microarray analyses showed several acquired abnormalities, including an LOH of the long arm of chromosome 7 and a duplication of the long arm of chromosome 4 (data not shown). FISH analyses confirmed the presence of an additional copy of the *TET2* locus in 20% of the nuclei in blood sample (data not shown). Sequencing of the PCR products obtained from single cells, sorted in individual wells from the fraction enriched in $CD34^-CD3^-CD19^-CD14^-$ tumor cells, confirmed the simultaneous presence of both *TET2* mutations in 6/10 assays (Figure 6D). We also PCR-amplified a fragment spanning the two mutations from the same tumor population, and the PCR products were subcloned using T/A vectors. Sequencing of individual bacterial colonies showed that a given mutation was always associated with a wild-type sequence at the other position. The P761fs/Q481wt combination was observed 24/42 times (57%) and the P761wt/Q481X combination 18/42 times (43%) (data not shown). No wild-type fragment was sequenced from these vectors, indicating that all three *TET2* copies present in the tumor cells were mutated. The observed ratio between both mutations indicated that the duplicated copy carried the P761fs mutation. In addition, these data indicate that the flow-sorted $CD34^-CD3^-CD19^-CD14^-$ fraction contained essentially tumor cells.

Additional genetic Alterations Are Associated with *TET2* Mutations

To identify additional genetic alterations in lymphomas, we used an exome sequencing approach to investigate DNA from the $CD34^-CD3^-CD19^-CD14^-$ (tumor) and $CD3^+$ (matched control) fractions. For each fraction, exonic DNA was captured using the SureSelect oligonucleotides (Agilent) and sequenced to generate 115600653 and 90633228 reads, from tumor and matched control libraries, respectively.

We first confirmed the presence of both *TET2* mutations in the tumor population at a ratio of 184/339 reads (54%) for P761fs and 140/389 reads (36%) for the Q481X, consistent with the duplication of the P761fs mutation (Figure 6E). The two mutations were observed at very low frequencies in the $CD3^+$ fraction (8/228 reads (4%) and 6/256 (2%) reads, respectively). We next looked for sequence variations, with respect to the human reference sequence, that were present only in the tumor population. Variations in seven genes (*IGSF21*, *CRIM1*, *CLSTN2*, *MCCC2*, *PLZF*, *ZC3H10*, and *ZNF774*) were validated by Sanger analysis (Figure 6E; Figure S6).

We then used quantitative RT-PCR to analyze the expression profile of the mutated genes in RNA from normal human brain, bone marrow, peripheral lymphocytes, and in flow-sorted tumor cells from patient 27 (Figure 6F). *CLSTN2* expression was observed in brain, but not in normal PBL, thymus, or bone marrow nor in patient's tumor samples (data not shown). The lack of detectable expression of *CLSTN2* in the hematopoietic system suggests that the *CLSTN2* mutation could be a passenger rather than a causal mutation. The transcription of *ZNF774*, *CRIM1*, and *IGSF21* was not detected in normal blood cells and/or in the tumor sample, but was observed in the bone marrow and/or thymus, questioning their role in the transformation process. Finally, we investigated the presence of the mutations in the $CD34^+$-derived colonies of the patient. Mutations in *PLZF* and *CRIM1* were identified in eight of eight $CD34^+$-derived colonies with the *TET2* P761fs mutation. The *ZNF774* mutation was observed in six of eight *TET2*-mutated colonies tested, suggesting that it occurred later in the transformation process than the three others (i.e., *TET2*, *PLZF*, and *CRIM1*). *ZNF774*, *PLZF*, and *CRIM1* mutations were not observed in 65 *TET2* wild-type $CD34^+$ colonies, suggesting that they did not occur independently of the *TET2* P761fs mutation.

DISCUSSION

The present study demonstrates the unique role of *Tet2* during murine hematopoiesis. Using two independent murine models,

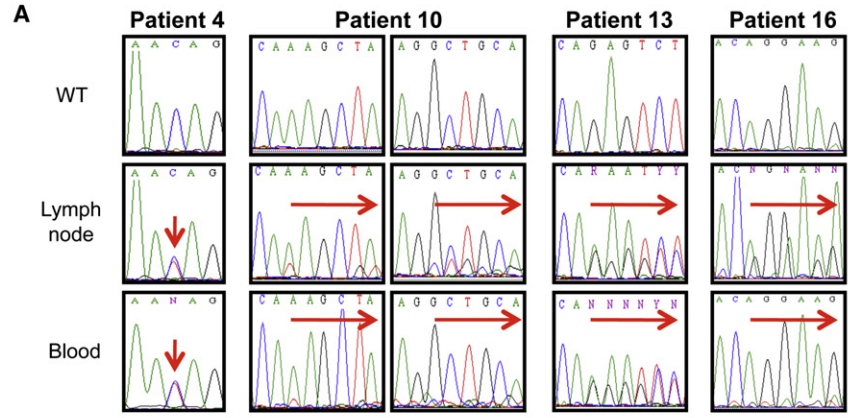

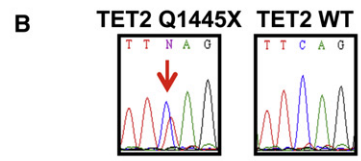

Q1445 X	WT	Total
6 (55%)	5	11

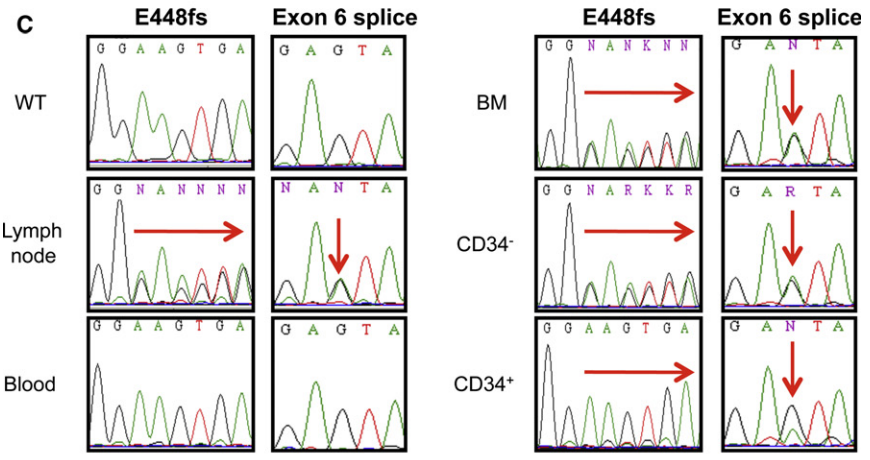

	E448fs/4663+1G>A	wt/4663+1G>A	wt/wt	Total
$CD34^+CD38^-$	8	5	6	**19**
$CD34^+CD38^+$	6	3	0	**9**
Total	**14**	**8**	**6**	**28**

Figure 5. *TET2* Mutation in Human T-Lymphoma Samples

(A) *TET2* sequence in diagnostic and matched control samples. Vertical arrows indicate the sequence variations. Other examples are shown in Figure S5. Horizontal arrows hang over the frameshift mutations. The presence of the mutated TET2 sequences was confirmed by sub cloning the PCR product from patient 10. The [1893_1896 delAAGC] (on the left) was observed on 1/29 DNA molecules analyzed and the [4527 delG] (on the right) was observed on 2/18 DNA molecules analyzed.

(B) Genotype of $CD34^+$ colonies from patient 8. Note that four erythroid lineage colonies were carrying the *TET2* mutation.

(C) Genotyping of diagnostic and purified bone marrow fractions and $CD34^+$ colonies from patient 2.

Left panel: *TET2* sequences at the lymphoma phase. Wild-type (WT) sequences are shown at the top. Node: nodal biopsy at diagnosis. Whole-blood sample was considered as normal matched DNA because it is devoid of IGH clonal marker.

Right panel: *TET2* sequences at the AML phase. BM: bone marrow nucleated cells. $CD34^-$: negative fraction after $CD34^+$ beads selection and $CD34^+$: flow-sorted $CD34^+$ population. Both mutations (frameshift [fs] and splice site mutation) are observed in all analyzed fractions.

Bottom: Genotype of colonies obtained from single cells sorted on CD34 and CD38 expression. 4663+1G > A would have appeared first in the course of the disease. Note that the cloning efficiency was extremely low (less than one colony out of 3000 seeded cells) and that colonies were small. See also Figure S5 and Table S2.

we showed that alteration of Tet2 function resulted in pleiotropic hematopoietic abnormalities and predisposed to development of a fatal disorder resembling human myeloid disorders in which *TET2* is mutated. In addition, these results led to a screen that identified *TET2* mutations as a recurrent event in several human lymphoid malignancies.

First, we show that complete inactivation of the catalytic domain of Tet2 (conditional model) lead to a reduction of the 5hmC marks in hematopoietic cells. It has been postulated that hmC might represent a step toward cytosine demethylation, but opposite data have been reported regarding the relation between hmC and mC levels in human samples (Figueroa et al., 2010; Ko et al., 2010a). It will be important to further investigate this point in the light of the recent description of *DNMT3A* mutation in human AML (Ley et al., 2010). *Tet2* also controls homeostasis of murine hematopoietic stem and progenitor cells, in keeping with the reported role of *TET2* in ES cell differentiation (Koh et al., 2011). Indeed, both *Tet2*-deficient models present an amplification of the hematopoietic stem/progenitor cell population in vivo associated with a competitive advantage in bone marrow transplantation assays and an increased self-renewal in vitro. Importantly, the gene-trap/hypomorph and conditional models exhibit some differences. For example, the gene-trap animals develop bona fide myeloid tumors that are transplantable to secondary recipients, whereas conditional animals did not develop fatal disease during the 15 months of follow-up. In keeping with the observation that *TET2* is mutated in half of human CMML patients

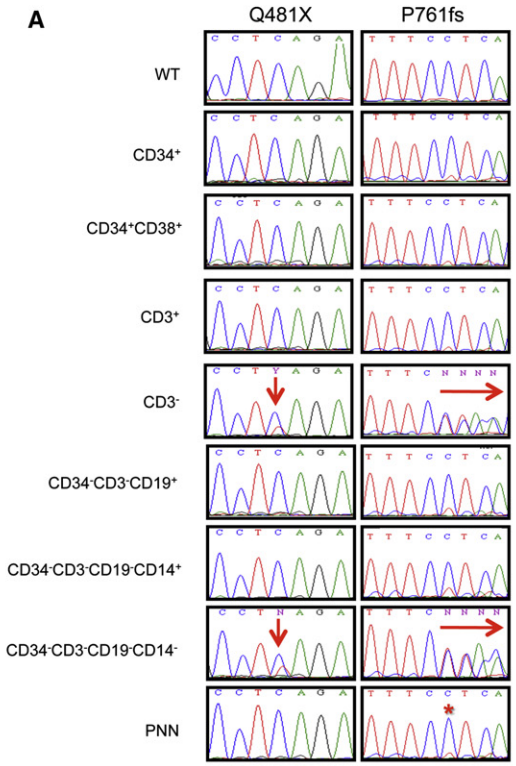

B

Fractions	Q481X	P761fs
$CD34^+$	-	-
$CD34^+CD38^+$	-	-
$CD3^+$	-	-
$CD3^-$	+	+
$CD34^-CD3^-CD19^+$	-	-
$CD34^-CD3^-CD19^-CD14^+$	-	-
$CD34^-CD3^-CD19^-CD14^-$	+	+
PNN	-	-

C

	P761fs/Q481wt	P761wt Q481wt	Total
$CD34^+$ colonies[1]	6 (7.1%)	78	**84**
$CD34^+$ colonies[2]	6 (6.5%)	87	**93**
$CD34^+CD38^-$ colonies[2]	1 (2.2%)	44	**45**

D

$CD34^-CD3^-CD19^-CD14^-$ cells	Q481X	P761fs
1	+	+
2	-	+
3	-	+
4	+	+
5	-	+
6	+	+
7	-	+
8	+	+
9	+	+
10	+	+

E

Gene	Localisation	Nucleotide change	Normal ($CD3^+$)	Tumour ($CD14^-$)	Mutation	Consequence	Prediction (Polyphen 2)
IGSF21	chr1 : 18692117-18692118	C>G	0/47 (0%)	19/37 (51%)	D314E	missense	probably damaging
CRIM1	chr2 : 36764605-36764606	C>T	1/62 (2%)	35/70 (50%)	T847I	missense	possibly damaging
CLSTN2	chr3 : 140167363-140167364	G>A	5/98 (5%)	48/118 (41%)	W266X	nonsense	no prediction
MCCC2	chr5 : 70939645-70939646	G>A	5/110 (5%)	57/122 (47%)	G358E	missense	probably damaging
ZBTB16/PLZF	chr11 : 114112936-114112937	C>T	5/51 (10%)	36/68 (53%)	A501V	missense	benign
ZC3H10	chr12 : 56514775-56514776	C>A	3/62 (5%)	36/84 (43%)	L144I	missense	probably damaging
ZNF774	chr15 : 90904097-90904098	DelC	1/106 (1%)	42/114 (37%)	P346fs	adds 80 aa before stop	no prediction
TET2	chr4 : 106 156 504-106 156 505	C>T	6/256 (2%)	140/389 (36%)	Q481X	nonsense	no prediction
TET2	chr4 : 106157378-106157379	DelC	8/228 (4%)	184/339 (54%)	P761fs	adds 51 aa before stop	no prediction

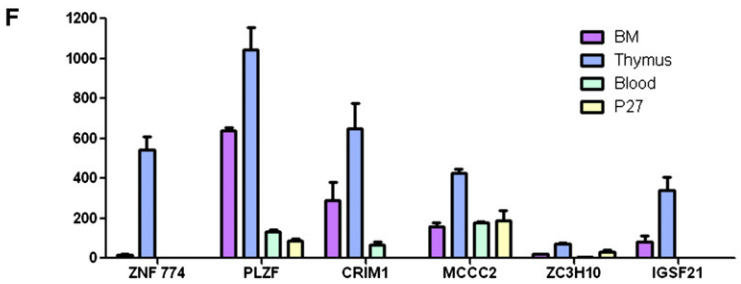

Figure 6. *TET2* and Other Acquired Mutations Are Found in Hematopoietic Progenitors

(A) *TET2* mutation status in flow-sorted subpopulations from blood samples from patient 27. The *TET2* sequences in sorted subpopulations are shown. Both mutations are detected in the $CD3^-$ and $CD34^-CD3^-CD19^-CD14^-$ populations, whereas only P761fs is observed as a trace (indicated by a star) in the other fractions.

(B) Summary of results presented in (A).

(Kohlmann et al., 2010; Kosmider et al., 2009b; Tefferi et al., 2009c), these results demonstrate that alteration of Tet2 functions contribute to the development of hematologic disorders with characteristics reminiscent of human CMML. Of note, we did not detect global alteration of 5hmC levels in the lineage$^-$ cells of the gene-trap model. It is possible that undetected subtle reduction of 5hmC marks is sufficient for the alteration of the hematopoietic progenitor compartment observed in both models. The observation that heterozygous animals present similar hematopoietic abnormalities supports this idea. However, we cannot exclude that susceptibility to transformation is controlled by another function of Tet2, as proposed recently for Tet1. Together, these results demonstrate that inactivation of Tet2 catalytic function and deregulation of 5hmC marks alter homeostasis of the hematopoietic progenitors and warrant further studies of *Tet2* expression level and structure in inactivation models.

Second, we observed that *Tet2* inactivation alters also T and B cell differentiation in mice. Of note, we observed the amplification of an aberrant CD19$^+$B220^{low} lymphoid population. We demonstrated that, in human malignancies, *TET2* is mutated in 2.0% of B cell, 11.9% of T cell lymphomas and ~30% of AITL samples. Extensive molecular and cellular analyses showed that *TET2* mutations are present in cells endowed with both myeloid and lymphoid potential in at least, a fraction of the *TET2*-mutated lymphoma patients. In some lymphoma patients, hematopoietic stem cells present mutation of one *TET2* allele in hematopoietic stem cells while lymphoma cells present mutation of both copies. Deep resequencing of the exome in a T cell lymphoma patient identified several mutations that are present with *TET2* mutation(s) either at the stem/progenitor cell level or only at latter steps of lymphoma development. Among those identified in early hematopoietic progenitor cells (i.e., *PLZF*, *CRIM1*, and *ZNF774*), PLZF has previously been shown to play a role in early hematopoietic progenitor biology (Dick and Doulatov, 2009). Although functional analyses will be required to assess the role of these mutations in lymphoma progression, these data suggest that *TET2* hemizygous mutation cooperates with additional mutations, including mutation of the second *TET2* copy. These findings suggest that in both mouse and human fine-tuning of *TET2* expression and activity is essential for normal homeostasis of the hematopoietic system and that loss of one allele of *TET2* contribute to disease development.

Finally, our results support the idea that disruption of Tet2 function leads to alteration of the homeostasis within the hematopoietic stem/progenitor compartment but per se does not induce a specific hematopoietic malignancy. We propose that Tet2 alteration, when it occurs in a stem/progenitor cell, predisposes to the development of malignancies in cooperation with secondary mutations that drives the phenotype of the disease. Combination of Tet2 deficiency with oncogenes, such as JAK2^{V617F}, will shed light on the oncogenic cooperation observed in human tumorigenesis.

EXPERIMENTAL PROCEDURES

Generation of the *Tet2*^{LacZ} and *Tet2*^{floxed} Alleles and Animal Analyses

Gene-trap mouse embryonic stem cell clone (SIGTR ES cell line AN0709: *Tet2*$^{Gt(AN0709)Wtsi}$, herein named *Tet2*^{LacZ}) carrying a β-galactosidase-neomycin (β-geo) resistance fusion cassette in *Tet2* gene were obtained from UC Davis Mutant Mouse Regional Resource Center (http://www.mmrrc.org) to generate gene-trap mouse line and the insertion of the β-geo cassette in intron 9 of *Tet2* was routinely genotyped on tail DNA by multiplexed polymerase chain reaction (PCR) using 5′-CAGCCAGGAAGACACTTACC-3′ and 5′-GACACCGATCTTGCTGGTTG-3′ primers into intron 9 to detect wild-type *Tet2* allele and 5′-CGCCTTGCAGCACATCCC-3′ and 5′-GGCCTTCCTGTA GCCAGC-3′ primers into the β-galactosidase sequence (and after the splicing donor site) to detect gene-trap allele (*Tet2*$^{LacZ/LacZ}$).

Mice harboring *Tet2* allele with exon 11 flanked by two *loxP* sites introduced in intron 10 and in the 3′ untranslated region of exon 11 (*Tet2*$^{Lox/Lox}$; "floxed allele") were generated by the Clinique de la Souris (Strasbourg, France) and intercrossed with mice expressing Cre recombinase under the control of the type I interferon-inducible Mx1 murine promoter (transgene referred as Mx1-Cre). PCR on tail DNA using 5′-GGCAGAGGCATGTTGAATGA-3′ and 5′-TAGACAAGCCCTGCAAGCAAA-3′ primers allowed to distinguish between wild-type and floxed allele. The *Tet2*^{Lox} allele was backcrossed into C57BL/6 background for at least six generations using speed-congenics (Harlan Laboratories) prior to analysis.

Acute inactivation of *Tet2* in 6- to 10-week-old Mx1-Cre$^+$*Tet2*$^{Lox/Lox}$ was performed by intraperitoneal injections (three injections every other day) of 800 μg poly(I:C)-LMW (InvivoGen, San Diego). Induction of Cre recombinase and efficient excision of floxed allele was confirmed by multiplex PCR using 5′-GGCAGAGGCATGTTGAATGA-3′, 5′-TAGACAAGCCCTGCAAGCAAA-3′ and 5′-GTGTCCCACGGTTACACACG-3′ primers that discriminated between floxed and deleted allele, respectively 305 and 237 bp. Therefore, we used the following nomenclature: Mx1-Cre$^+$*Tet2*$^{Lox/Lox}$ = *Tet2*$^{-/-}$, Mx1-Cre$^-$*Tet2*$^{Lox/Lox}$ = *Tet2*$^{+/+}$.

Competitive transplantations were performed by transplanting equal numbers of total bone marrow cells from CD45.1$^-$CD45.2$^+$ *Tet2*-deficient and CD45.1$^+$CD45.2$^+$ wild-type animals into lethally irradiated CD45.1$^+$CD45.2$^-$ recipients. For LSK cells transplantation, LSK cells were purified by flow cytometry from *Tet2*-deficient animals and 4000 LSK cells supplemented with 1 × 10^6 total bone marrow cells from wild-type were injected to lethally irradiated recipients. Expression of CD45.1 and CD45.2 was followed by flow cytometry on blood cells every month and animals were analyzed at 4 months after transplantation.

Animal experiments were conducted according to the Institut Gustave Roussy Institutional guidelines and authorized by the Direction Départementale des Services Vétérinaires du Val de Marne.

Patient Samples Collection

Lymph node, peripheral blood, and bone marrow samples from the patients were obtained with their informed consent and the approval of the local Research Ethics Committees (Centre Henri Becquerel, Pitié-Salpétrière, and Cochin hospitals). Additional information on patient samples is available in Tables S2 and S3.

(C) Genotype of colonies obtained from sorted single CD34$^+$ cells. [1] and [2] correspond to two successive blood samples at a 4-month interval. Only the P761fs mutation is observed in CD34$^+$ (~7%) and CD34$^+$CD38$^-$ (2.2%) colonies. No P761fs positive colony was observed out of 40 CD34$^+$CD38$^+$ single-cell-derived colonies (data not shown).
(D) Single-cell analyses show the presence of both *TET2* mutations in the same cell.
(E) Somatic mutations identified through exome analyses of patient 27.
(F) Expression level of the mutated genes in normal tissues and tumor sample. Expression levels were normalized with respect to *GUSB* expression.
See also Figure S6 and Table S3.

Flow Cytometry, Cell Sorting, and Purification

Total white blood cells, obtained from peripheral blood after lysis of red blood cells, and single-cell suspensions from bone marrow, spleen and thymus were stained in toto in PBS supplemented with 2% fetal bovine serum (FBS) with fluorochrome-conjugated mouse antibodies raised against specific markers of hematopoietic lineages (BD Biosciences PharMingen, except otherwise mentioned). Additional information on antibody clones is available in Supplemental Methods. Viability of cells was confirmed by using the Sytox Blue (Invitrogen) viability marker. Flow cytometric analysis and cell sorting were performed using a FACSCantoII Flow Cytometer (BD Biosciences) and a MoFlow (Becton Dickinson) or a FACSAriaIII (BD Biosciences), respectively. Immunophenotypic data were analyzed using the FlowJo Version 7.2.4 software (TreeStar).

For human samples, bone marrow or peripheral blood mononuclear cells, lymphocytes, and granulocytes were isolated and stored in liquid nitrogen as viable cells in FBS with 10% dimethyl-sulfoxide (DMSO, Sigma). Patients were selected on DNA availability. Their clinical and biological characteristics are summarized in Table S2. Diagnoses were made by standard international criteria. Cells were purified using Miltenyi beads according the manufacturer instructions. When mentioned, cells were sorted after labeling with PE–CD34 and APC–CD38 antibodies (Immunotech) using a FACSDiva cell sorter (Becton Dickinson).

In Vitro Clonogenic Assays

Sorted $CD34^+$ cells were seeded at one cell per well on methylcellulose in MEM alpha medium supplemented with 10% FBS (Stem Cell Technologies), and a cocktail of early cytokines (thrombopoietin [TPO], interleukin [IL-3], Flt3-L, Stem Cell Factor [SCF], erythropoietin [EPO], granulocyte-colony stimulating factor [G-CSF], granulocyte/macrophage-colony stimulating factor [GM-CSF] and IL-6). After 2 weeks, individual clones were collected for further genotyping.

For patient 2, total mononuclear cells were seeded in 2% standard methylcellulose supplemented with 25% FBS (Stem Cell Technologies), and a cocktail of cytokines as described.

Nucleic Acid Methods

DNA and RNA were extracted using commercial kits (QIAGEN or Roche). Polymerase chain reaction (PCR) and direct sequencing reaction were performed using standard conditions with primers available upon request. Nucleotide sequences were compared to wild-type human genomic sequence present in the databases (genome.ucsc.edu). All observed mutations were scored on both strands. Additional information on exome sequencing is available in Supplemental Experimental Procedures.

In Vitro Differentiation Assays

LSKs (5×10^2), total BM (5×10^4), and spleen cells (5×10^4) isolated from mutant or control mice were cultured in methylcellulose-based medium (MethoCult M3434; StemCell Technologies) and scored for CFUs (colony-forming units) using combined scoring for burst-forming unit erythroids (BFU-Es), CFU-megakaryocytes (CFU-Mks), CFU-granulocyte macrophages (CFU-GMs), and CFU-granulocyte erythroid macrophage megakaryocytes (CFU-GEMMs) after 7 days. All live colonies were counted for each of the two 35 mm dishes plated per sample.

Quantitative PCR

cDNA was synthesized from total RNA purified (using the RNeasy microkit, QIAgen) from sorted LSK, common myeloid progenitor (CMP), megakaryocyte-erythrocyte progenitor (MEP), and granulocyte-macrophage progenitor (GMP) populations using the Superscript II reverse transcriptase (Invitrogen). TaqMan probes were purchased from Applied Biosystems (*Tet1*: Mm01169089; *Tet2* [exon 9–10]: Mm00524395_m1; *Tet2* [exon 10–11]: Mm01312907; *Tet3*, Mm01184936; *Abl1*, Mm00802038). *Tet2* (exon 3–4) transcript were detected using the following primers; Primer1: 5′-agaatcagatactcctggtgaacaaa-3′, Primer2: 5′-cctagatgggtataataaggagcttcat-3′, Probe: 5′ FAM-tctggattgcatccttcacatttgccat-3′TAM. *Tet2-LacZ* fusion transcript was detected using the following primers and probe; Primer1 (*Tet2* exon 9): 5′-cccacagagaccagcagaaca-3′, Primer2 (*LacZ*): 5′-tgcgttcttcttctttggttttc-3′, Probe: 5′FAM-cctgggaccactgtactgccatttgg-3′TAM. The expression level of each gene was assessed by qRT-PCR with an ABI PRISM 7500 and calculated following the ΔΔCt method; each sample was analyzed in triplicate and normalized with *Abl1* and *GusB* expression (Applied Biosystems Mm00802038_g1 and Mm03003537_s1, respectively).

Statistical and Quantification Analyses

Results are expressed as mean values ± SEM. Statistical significance of differences between the results was assessed using a 2-tailed unpaired Student's t test, performed using Prism (GraphPad software, version 5.03). p values < 0.05 were considered statistically significant. Quantification of the 5mC and 5hmC signals was performed by dot-blotting DNA and using antibodies from Eurogentec (1/500 dilution) and Active Motif (1/10,000 dilution) respectively. Signal was quantified using GelEval (FrogDance software, version 1.32).

ACCESSION NUMBERS

Microarray procedures and data used in this publication have been deposited in the European Bioinformatics Institute (EBI) database with the following accession number: E-TABM-1161.

SUPPLEMENTAL INFORMATION

Supplemental Information includes six figures, three tables, and Supplemental Experimental Procedures and can be found with this article online at doi:10.1016/j.ccr.2011.06.003.

ACKNOWLEDGMENTS

We thank Dr. R. L. Levine and Omar Abdel-Wahab for valuable help with resequencing, Dr. Paola Rivera-Munhoz and Dr. Sophie Ezine for helpful discussions, and Olivia Bawa for histopathological analysis. The work was funded by grants from INSERM, Institut National du Cancer (INCa), Ligue Nationale Contre le Cancer (LNCC), Association de Recherche contre le Cancer (ARC), Fondation Gustave Roussy and by NIH/NCI grants CA129831 and CA129831-03S1 (L.G.). C.Q. is the recipient of a fellowship from the region île de France.

Received: February 24, 2011
Revised: May 12, 2011
Accepted: June 8, 2011
Published online: June 30, 2011

REFERENCES

Abdel-Wahab, O., Mullally, A., Hedvat, C., Garcia-Manero, G., Patel, J., Wadleigh, M., Malinge, S., Yao, J., Kilpivaara, O., Bhat, R., et al. (2009). Genetic characterization of TET1, TET2, and TET3 alterations in myeloid malignancies. Blood *114*, 144–147.

Abdel-Wahab, O., Manshouri, T., Patel, J., Harris, K., Yao, J., Hedvat, C., Heguy, A., Bueso-Ramos, C., Kantarjian, H., Levine, R.L., and Verstovsek, S. (2010). Genetic analysis of transforming events that convert chronic myeloproliferative neoplasms to leukemias. Cancer Res. *70*, 447–452.

Beer, P.A., Delhommeau, F., Lecouedic, J.P., Dawson, M.A., Chen, E., Bareford, D., Kusec, R., McMullin, M.F., Harrison, C.N., Vannucchi, A.M., et al. (2010). Two routes to leukemic transformation following a JAK2 mutation-positive myeloproliferative neoplasm. Blood *115*, 2891–2900.

Couronné, L., Lippert, E., Andrieux, J., Kosmider, O., Radford-Weiss, I., Penther, D., Dastugue, N., Mugneret, F., Lafage, M., Gachard, N., et al. (2010). Analyses of TET2 mutations in post-myeloproliferative neoplasm acute myeloid leukemias. Leukemia *24*, 201–203.

Cozzio, A., Passegué, E., Ayton, P.M., Karsunky, H., Cleary, M.L., and Weissman, I.L. (2003). Similar MLL-associated leukemias arising from self-renewing stem cells and short-lived myeloid progenitors. Genes Dev. *17*, 3029–3035.

Delhommeau, F., Dupont, S., Della Valle, V., James, C., Trannoy, S., Massé, A., Kosmider, O., Le Couedic, J.P., Robert, F., Alberdi, A., et al. (2009). Mutation in TET2 in myeloid cancers. N. Engl. J. Med. *360*, 2289–2301.

Dick, J.E. (2008). Stem cell concepts renew cancer research. Blood *112*, 4793–4807.

Dick, J.E., and Doulatov, S. (2009). The role of PLZF in human myeloid development. Ann. N. Y. Acad. Sci. *1176*, 150–153.

Figueroa, M.E., Abdel-Wahab, O., Lu, C., Ward, P.S., Patel, J., Shih, A., Li, Y., Bhagwat, N., Vasanthakumar, A., Fernandez, H.F., et al. (2010). Leukemic IDH1 and IDH2 mutations result in a hypermethylation phenotype, disrupt TET2 function, and impair hematopoietic differentiation. Cancer Cell *18*, 553–567.

Goardon, N., Marchi, E., Atzberger, A., Quek, L., Schuh, A., Soneji, S., Woll, P., Mead, A., Alford, K.A., Rout, R., et al. (2011). Coexistence of LMPP-like and GMP-like leukemia stem cells in acute myeloid leukemia. Cancer Cell *19*, 138–152.

Huntly, B.J., Shigematsu, H., Deguchi, K., Lee, B.H., Mizuno, S., Duclos, N., Rowan, R., Amaral, S., Curley, D., Williams, I.R., et al. (2004). MOZ-TIF2, but not BCR-ABL, confers properties of leukemic stem cells to committed murine hematopoietic progenitors. Cancer Cell *6*, 587–596.

Ito, S., D'Alessio, A.C., Taranova, O.V., Hong, K., Sowers, L.C., and Zhang, Y. (2010). Role of Tet proteins in 5mC to 5hmC conversion, ES-cell self-renewal and inner cell mass specification. Nature *466*, 1129–1133.

Jaffe, E.S. (2009). The 2008 WHO classification of lymphomas: implications for clinical practice and translational research. Hematology Am. Soc. Hematol. Educ. Program, 523–531.

Jankowska, A.M., Szpurka, H., Tiu, R.V., Makishima, H., Afable, M., Huh, J., O'Keefe, C.L., Ganetzky, R., McDevitt, M.A., and Maciejewski, J.P. (2009). Loss of heterozygosity 4q24 and TET2 mutations associated with myelodysplastic/myeloproliferative neoplasms. Blood *113*, 6403–6410.

Jones, D. (2010). Functional classification of peripheral T-cell lymphomas as an approach to improve outcome prediction and therapy selection. Semin. Hematol. *47* (*Suppl 1*), S1–S4.

Ko, M., Huang, Y., Jankowska, A.M., Pape, U.J., Tahiliani, M., Bandukwala, H.S., An, J., Lamperti, E.D., Koh, K.P., Ganetzky, R., et al. (2010a). Impaired hydroxylation of 5-methylcytosine in myeloid cancers with mutant TET2. Nature *468*, 839–843.

Ko, M., Huang, Y., Jankowska, A.M., Pape, U.J., Tahiliani, M., Bandukwala, H.S., An, J., Lamperti, E.D., Koh, K.P., Ganetzky, R., et al. (2010b). Impaired hydroxylation of 5-methylcytosine in myeloid cancers with mutant TET2. Nature *468*, 839–843.

Kohlmann, A., Grossmann, V., Klein, H.U., Schindela, S., Weiss, T., Kazak, B., Dicker, F., Schnittger, S., Dugas, M., Kern, W., et al. (2010). Next-generation sequencing technology reveals a characteristic pattern of molecular mutations in 72.8% of chronic myelomonocytic leukemia by detecting frequent alterations in TET2, CBL, RAS, and RUNX1. J. Clin. Oncol. *28*, 3858–3865.

Koh, K.P., Yabuuchi, A., Rao, S., Huang, Y., Cunniff, K., Nardone, J., Laiho, A., Tahiliani, M., Sommer, C.A., Mostoslavsky, G., et al. (2011). Tet1 and Tet2 regulate 5-hydroxymethylcytosine production and cell lineage specification in mouse embryonic stem cells. Cell Stem Cell *8*, 200–213.

Kosmider, O., Gelsi-Boyer, V., Cheok, M., Grabar, S., Della-Valle, V., Picard, F., Viguié, F., Quesnel, B., Beyne-Rauzy, O., Solary, E., et al; Groupe Francophone des Myélodysplasies. (2009a). TET2 mutation is an independent favorable prognostic factor in myelodysplastic syndromes (MDSs). Blood *114*, 3285–3291.

Kosmider, O., Gelsi-Boyer, V., Ciudad, M., Racoeur, C., Jooste, V., Vey, N., Quesnel, B., Fenaux, P., Bastie, J.N., Beyne-Rauzy, O., et al; Groupe Francophone des Myélodysplasies. (2009b). TET2 gene mutation is a frequent and adverse event in chronic myelomonocytic leukemia. Haematologica *94*, 1676–1681.

Kriaucionis, S., and Heintz, N. (2009). The nuclear DNA base 5-hydroxymethylcytosine is present in Purkinje neurons and the brain. Science *324*, 929–930.

Langemeijer, S.M., Kuiper, R.P., Berends, M., Knops, R., Aslanyan, M.G., Massop, M., Stevens-Linders, E., van Hoogen, P., van Kessel, A.G., Raymakers, R.A., et al. (2009). Acquired mutations in TET2 are common in myelodysplastic syndromes. Nat. Genet. *41*, 838–842.

Ley, T.J., Ding, L., Walter, M.J., McLellan, M.D., Lamprecht, T., Larson, D.E., Kandoth, C., Payton, J.E., Baty, J., Welch, J., et al. (2010). DNMT3A mutations in acute myeloid leukemia. N. Engl. J. Med. *363*, 2424–2433.

Nibourel, O., Kosmider, O., Cheok, M., Boissel, N., Renneville, A., Philippe, N., Dombret, H., Dreyfus, F., Quesnel, B., Geffroy, S., et al. (2010). Incidence and prognostic value of TET2 alterations in de novo acute myeloid leukemia achieving complete remission. Blood *116*, 1132–1135.

Saint-Martin, C., Leroy, G., Delhommeau, F., Panelatti, G., Dupont, S., James, C., Plo, I., Bordessoule, D., Chomienne, C., Delannoy, A., et al; French Group of Familial Myeloproliferative Disorders. (2009). Analysis of the ten-eleven translocation 2 (TET2) gene in familial myeloproliferative neoplasms. Blood *114*, 1628–1632.

Schaub, F.X., Looser, R., Li, S., Hao-Shen, H., Lehmann, T., Tichelli, A., and Skoda, R.C. (2010). Clonal analysis of TET2 and JAK2 mutations suggests that TET2 can be a late event in the progression of myeloproliferative neoplasms. Blood *115*, 2003–2007.

Tahiliani, M., Koh, K.P., Shen, Y., Pastor, W.A., Bandukwala, H., Brudno, Y., Agarwal, S., Iyer, L.M., Liu, D.R., Aravind, L., and Rao, A. (2009). Conversion of 5-methylcytosine to 5-hydroxymethylcytosine in mammalian DNA by MLL partner TET1. Science *324*, 930–935.

Tefferi, A., Levine, R.L., Lim, K.H., Abdel-Wahab, O., Lasho, T.L., Patel, J., Finke, C.M., Mullally, A., Li, C.Y., Pardanani, A., and Gilliland, D.G. (2009a). Frequent TET2 mutations in systemic mastocytosis: clinical, KITD816V and FIP1L1-PDGFRA correlates. Leukemia *23*, 900–904.

Tefferi, A., Lim, K.H., Abdel-Wahab, O., Lasho, T.L., Patel, J., Patnaik, M.M., Hanson, C.A., Pardanani, A., Gilliland, D.G., and Levine, R.L. (2009b). Detection of mutant TET2 in myeloid malignancies other than myeloproliferative neoplasms: CMML, MDS, MDS/MPN and AML. Leukemia *23*, 1343–1345.

Tefferi, A., Lim, K.H., Abdel-Wahab, O., Lasho, T.L., Patel, J., Patnaik, M.M., Hanson, C.A., Pardanani, A., Gilliland, D.G., and Levine, R.L. (2009c). Detection of mutant TET2 in myeloid malignancies other than myeloproliferative neoplasms: CMML, MDS, MDS/MPN and AML. Leukemia *23*, 1343–1345.

Tefferi, A., Pardanani, A., Lim, K.H., Abdel-Wahab, O., Lasho, T.L., Patel, J., Gangat, N., Finke, C.M., Schwager, S., Mullally, A., et al. (2009d). TET2 mutations and their clinical correlates in polycythemia vera, essential thrombocythemia and myelofibrosis. Leukemia *23*, 905–911.

Viguié, F., Aboura, A., Bouscary, D., Ramond, S., Delmer, A., Tachdjian, G., Marie, J.P., and Casadevall, N. (2005). Common 4q24 deletion in four cases of hematopoietic malignancy: early stem cell involvement? Leukemia *19*, 1411–1415.